Selective and Sensitive Room Temperature Detection of Ammonia by PPy-Ag Nanocomposite

Dattatray M. Nerkar

Sathaye College, Dixit Road, Vile Parle (East), Mumbai 400057, India

Abstract: This paper describes synthesis of polypyrrole-silver nanocomposite (PPy-Ag-NC) via in situ chemical oxidative polymerization of pyrrole, based on colloidal suspension of silver nanoparticles. The structure analysis of synthesized nanocomposite was done by Fourier transform infrared (FTIR) spectroscopy. Transmission electron microscopy (TEM) micrographs showed spherical Ag nanoparticles of about 38-60 nm were embedded in the PPy matrix. Scanning Electron Microscopy (SEM) photo graphs revealed formation of uniform granular morphology. X-ray diffraction (XRD) pattern shows broad peak at $2\theta = 25.3o$ suggesting that PPy is amorphous, but peaks at 2θ values of 38.2°, 44.5°, 64.3° and 78.4° corresponding to face centered cubic silver. Room temperature ammonia gas sensing behaviour of PPy-Ag nanocomposite films were examined. Gas sensing tests demonstrated that the composite films exhibited a fast response (58s to 153s), rapid recovery (347s to 746s) and high sensitivity and sensitivity at room temperature with a detection of low concentration (50 to 500 ppm) of ammonia gas. The experimental result demonstrates the potential of using PPy-Ag nanocomposite as sensing material for the fabrication of room temperature operating ammonia sensor.

Keywords: Polypyrrole, Silver nanoparticles colloid, Nanocomposite, in situ Polymerization, Ammonia, Gas Sensing

I. INTRODUCTION

Conceptual origin of nanotechnology was introduced by the physicist Richard Feynman in a lecture entitled 'There's plenty of room at the bottom' in December 1959, at an annual meeting of the American Physical Society. Nanocomposites have created a new class of materials that exhibit unique physical and chemical properties making them suitable for applications in various fields. The nanocomposite materials of plasmonic nanoparticles like Ag, Au etc. were widely studied in the past few years due to their collaborative properties which considerably differ from their single-component counterpart.

Polypyrrole (PPy) is one of the promising conducting polymers due to its high conductivity, ease of preparation, good environmental stability and a variety of applications which makes it suitable for preparation of nanocomposites [1, 2]. Nanomaterials-based sensors have been considered to be a promising gas sensing tool due to their large surface–to–volume ratio, controllable structure and easily tailored chemical and physical properties. This result in high sensitivity, fast dynamic process and even increased specificity.

In recent years, few sensors based on nanostructured conducting polymers/nanocomposites to detect different kinds of gases have been developed. Most of which have been reviewed by Sih et al. [3] and Rajesh et al. [4].Yang et al. [5] have demonstrated the synthesis of PPy-Ag nanocomposite by in situ reduction process. Ag nanoparticles were uniformly absorbed onto the surface of PPy in the presence of Polyvinylpyrrolidone (PVP). They have studied the response of this PPy-Ag nanocomposite to NH_3 gas by observing the change in the resistance of the nanocomposites. The sensors based on the PPy-Ag nanocomposite presented excellent reversibility and reproducibility in response even at a ppm level. Kate et al. [6] have described the polymerization of pyrrole by thermal polymerization in the presence of silver ions, using silver nitrate in order to synthesize PPy-Ag nanocomposite. The PPy-Ag nanocomposite so prepared has been tested for its gas sensing for various gases. They have reported the sensing behaviour of PPy-Ag film with temperature, at 100^oC the thick acts as NH_3 sensor, but the same film identifies H_2S at 250^oC. Detection of ammonia can be done using metal oxide gas sensor, catalytic gas sensor, conducting polymers, spectrophotometric ammonia detector and optical absorption ammonia detector.

Ammonia (Azane), is a colourless gas with a sharp, penetrating pungent smell. It is the simplest inorganic base and an important source of nitrogen for many applications. The major part of ammonia produced is used in agriculture as fertilizer. It is also utilized as a refrigerant gas, for purification of water supply, explosives, textiles and west water treatment. Inspite of being commonly found in nature and used widely, ammonia happens to be hazardous and caustic in its concentrated form. Inhalation of lower concentrations can cause burning of the eyes, nose and throat irritation. Exposure to high concentrations of ammonia can result in

blindness, lung damage or death [7-9]. Hence, early detection and monitoring of ammonia in environment are required for a wide range of applications.

Chemical functionalization is a simple and cost-effective technique which offers spatially-tailored functionalization.This work is an attempt to present the synthesis of polypyrrole-silver nanocomposite (PPy-Ag-NC) via in situ chemical oxidative polymerization of pyrrole, based on citrate reduced colloidal suspension of silver nanoparticles and its ammonia sensing properties

II. MATERIALS & METHODS

A. Materials and Reagents

Pyrrole (Spectrochem Pvt. Ltd.) Ferric Chloride (anhydrous) and Trisodium Citrate (S. D. Fine Chem. Ltd.) and Silver Nitrate (Research Lab Fine Chem. Industries) were used for polymer and nanocomposite synthesis. Monomer- Pyrrole was purified by double distillation prior to synthesis. Deionised water was used for all synthesis. All chemicals were of analytical graded pure and used without any further purification.

Gas canisters, along with fixed pressure regulator (C10 valve) having outflow rate 0 to 0.5 LPM, were purchased from Chemtron Science laboratories Pvt. Ltd.,, Mumbai. All the portable calibration gas (CALIPORT) mixtures of 1000 ppm of impurity gases in N_2 environment, were 0.5 LTR aluminium high- pressure canisters.

B. Synthesis of Polypyrrole (PPy)

Polypyrrole (PPy) was synthesized by in situ doping polymerization method, the details of the technique are described elsewhere [10,11]. In brief, to the monomer (pyrrole) solutions in a beaker, oxidizing agent ($FeCl_3$) was added dropwise with constant stirring at low temperature (0-3°C). The synthesis was allowed to proceed for 3 hours at 0-3°C for complete polymerisation. The mixture was kept overnight without agitation at room temperature in a sealed container. The precipitate was collected by vacuum filtration, the product was rinsed with double distilled water many times and dried under vacuum.

C. Synthesis of Silver Nanoparticles (Ag NP)

The synthesis of Silver Nanoparticles was done using Turkevich method, the experimental details has been reported in our previous papers [12]. In a typical procedure for the preparation of Ag NP, aqueous 1 nm solution of $AgNO_3$ and 10 nM trisodium citrate solutions were prepared. Silver nitrate solution was heated to boil in which trisodium citrate solution was added dropwise with vigorously stirring at boiling temperature. The solution changes from colorless to golden yellow confirming formation of silver nanoparticles [13]. The colloidal solution was cooled to room temperature.

D. Synthesis of Polypyrrole-Silver Nanocomposite (PPy-Ag NC)

The PPy-Ag NC was synthesized by in situ chemical oxidative polymerization, the experimental details has been reported in our previous publication [12]. In short, 100 ml of Ag NPs colloidal solution was cooled in a beaker kept in an ice bath and stirred by a magnetic stirrer. Required quantity of pyrrole was added via syringe to this solution followed by drop by drop addition of aqueous $FeCl_3$ solution. The colour of the solution changed from pale yellow to black. The reaction was carried out for 3h under the same parameters. The solution was kept unagitated for 48 h in a sealed container at room temperature. The precipitate was collected by vacuum filtration, the product was rinsed with double distilled water many times and dried under vacuum [14, 15].

E. Material characterization

The chemical structure of PPy and PPy-Ag NC was analyzed by Fourier Transform Infra-Red (FTIR) spectroscopy (Perkin-Elmer Ltd. S:2000) in the 400–4000 cm^{-1} frequency range. The surface microstructure was investigated using scanning electron microscope (JEOL, JSM-7600F) and transmission electron microscope (JEOL, JEM-2100F) The XRD patterns for the structural analysis were recorded using Philips Panalytical X'Pert over the range of $2\theta = 20^0$ to 80^0.

F. Fabrication of sensor

The sensor consisting of an interdigitated electrodes (IDE) with a layer of PPy-Ag NC coated on top. The IDE consisted of PCB having five pairs of Cu tracks printed onto an epoxy glass substrate. The width of the track and the gap between two successive tracks were 1 mm each. The size of the entire device was 30 mm × 20 mm [9, 16]. 10mg of PPy-Ag NC powder was dissolved in m-cresol and sonicated for 10 min. to form a paste. The paste was then brush-coated on the IDE epoxy glass substrates to form films. Films were dried at 40 ^{o}C for 24 h and used to evaluate the sensing characteristics. The schematic diagram of a fabricated sensor and its photograph is shown in Fig. 1.
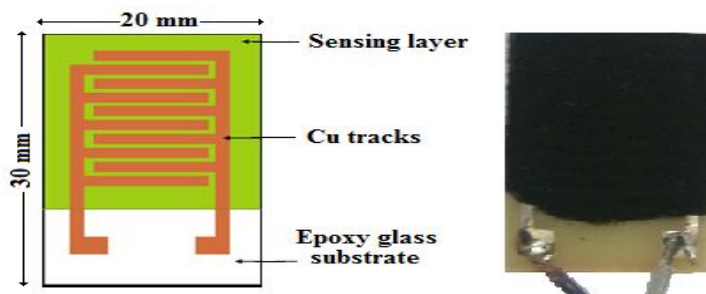
Fig. 1: Schematic diagram of a fabricated sensor and photograph of the fabricated sensor

G. Gas sensing measurements

For measuring the gas response, a specially prepared gas chamber (500 cm³) was used. Gas sensing measurements were performed in a static mode. The fabricated sensor was mounted in the gas chamber. The schematic diagram of a typical gas sensing unit is shown in Fig. 2. The measured quantity of test gas was injected with the help of a syringe to get desired gas concentration (ppm) in the chamber. The electrical resistance was measured by using Scientific Programmable Digital Multimeter (SM5015) which was connected to computer for data acquisition. Once steady state was achieved, recovery of the sensor was recorded by exposing the sensor to fresh air. This was done by opening both the inlet and outlet valves (V_1 and V_2) of the chamber simultaneously. At the same time, the vacuum pump was switched on. Inlet valve (V_1) allowed fresh air to enter the chamber while outlet valve (V_2) allowed the gas to exit the chamber. The vacuum pump accelerated the process of degassing. All the gas sensitivity measurements were carried out at room temperature.

The performance of the sensor was evaluated using:

$$Sensitivity\ (S)\% = \frac{R_{air} - R_{gas}}{R_{air}} \times 100\ \% = \frac{\Delta R}{R_{air}} \times 100\ \% \tag{1}$$

where R_{air} is the electrical resistances of the sensor in test gas and R_{gas} resistances in clear air. Response time is the time taken for the sensor to attain 90% of the maximum change in resistance on exposure to test gas. Recovery time is the time taken by the sensor to get back 90% of the original resistance after degassing [17].
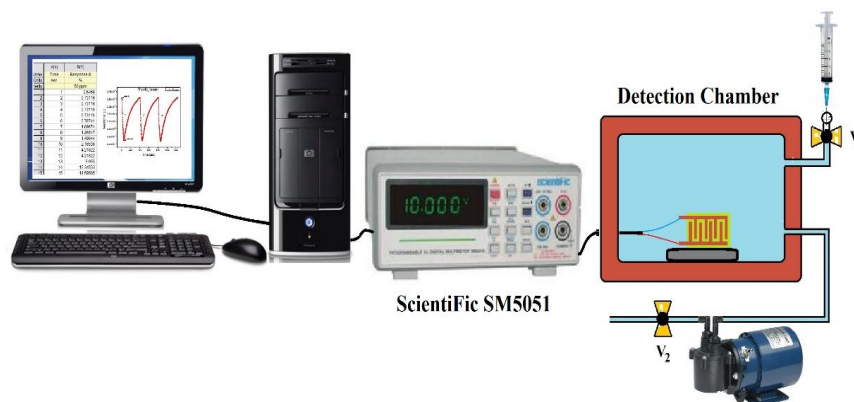

Fig. 2: Schematic diagram of a gas sensing experimental setup.

III.RESULTS & DISCUSSION

A. Fourier transform infrared (FTIR) analysis

The presence of a series of IR characteristic bands for pure PPy and PPy-Ag nanocomposite is shown in Fig. 3. The FTIR spectrum of PPy [3(a)] shows absorption bands at 3430.3 cm⁻¹ (N–H stretching), 1695 cm⁻¹ (C=N bonds), 1539.5 cm⁻¹ (Ring stretching mode C=C, C–C), 1459.4 cm⁻¹ (C–H out-plane deformation), 1300.5 cm⁻¹ (=C–H in plane vibration), 1050 cm21 (ONH bending deformation), 778.9 - 1086.8 cm⁻¹ (= C-H in plane deformation vibration), 675 cm⁻¹ (C-C out of plane ring deformation or C-H rocking), 611.2 cm⁻¹ (C–H wagging). All observed absorption bands are in agreement with literature results [18-20]. Fig. 3(b) shows the FTIR spectrum of PPy-Ag nanocomposite. It is similar to pure PPy with positions of the peaks shifted to a higher wavenumber. The shift can be attributed to the coordination of silver with the polymer and over oxidation of PPy [21-23].
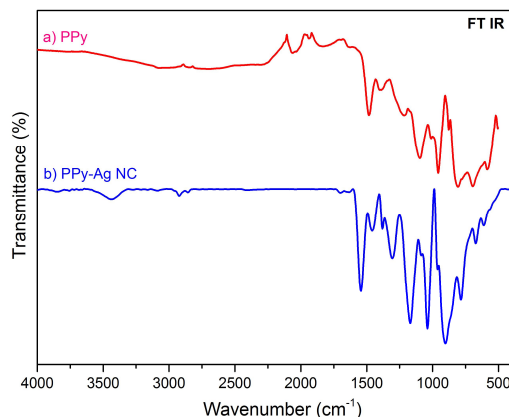
Fig. 3: FTIR Spectra of PPy and PPy-Ag nanocomposite.

B. Scanning electron microscopy (SEM) analysis

The microstructure of polypyrrole is shown in Fig. 4(a). It has uniform globular structure and the average size of the globules is found to be 6-19 μm. The observed granules were nearly spherical in shape and have a close packing structure. It was also observed that these spherulites form a continuous structure by growing over one another. A typical SEM image of the PPy-Ag nanocomposite is shown in Fig. 4(b), which suggests that the product exhibits a globular structure with a diameter about 180 -300 nm [24]. The globular structure is suitable for gas sensing applications as it endorses adsorption of gas molecules [25].
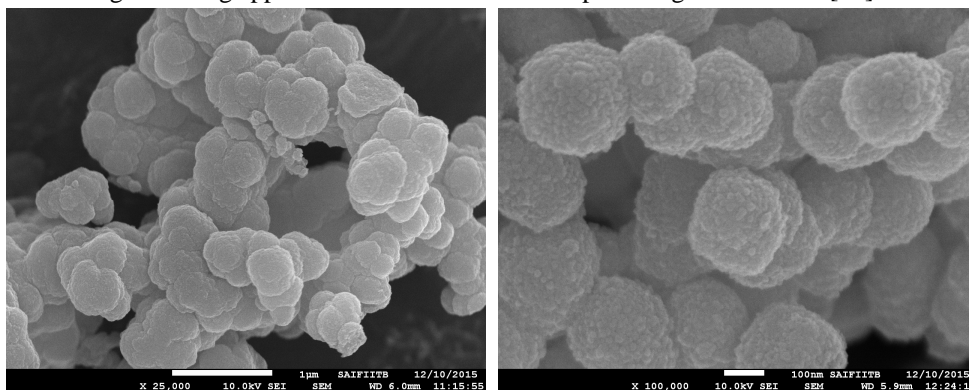

Fig. 4: SEM images of (a) PPy and (b) PPy-Ag nanocomposite.

C. Transmission electron microscopy (TEM) analysis

Transmission electron microscopy micrographs of the PPy-Ag nanocomposites with different magnification are shown in Fig. 5. It is observed that the small black particles are incorporated into the PPy matrix as shell structure. The Ag nanoparticles seem to be embedded in the PPy matrix. The preparation method produced spherical/semispherical silver nanoparticles with average size of 40 ± 5 nm. The results obtained from TEM clearly reveal that Ag nanoparticles are separated and are not uniform, which is probably due to aggregation or clustering of the nanoparticles. [26].
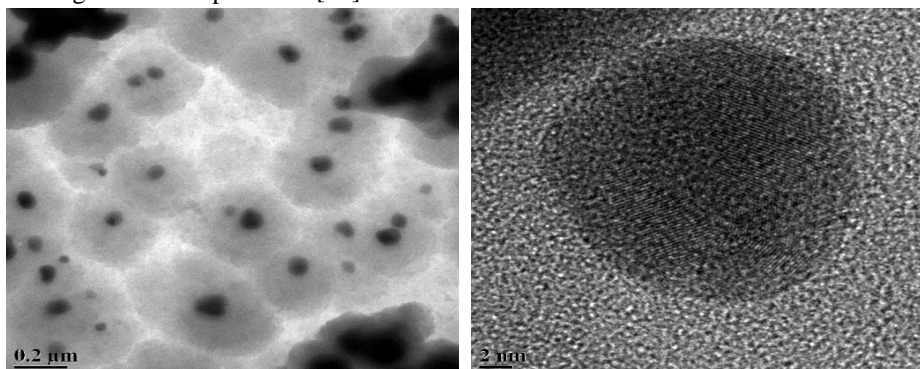

Fig. 5: TEM images of PPy-Ag nanocomposite.

D. XRD analysis

The XRD patterns of PPy and PPy-Ag nanocomposite are presented in Fig. 6. Broad peak observed at $2\theta = 25.3^0$ [Fig. 6(a)] is ascribed to the amorphous characteristic of PPy [27]. The XRD of PPy-Ag nanocomposite [Fig. 6(b)] shows, decrease in the broadness of the amorphous peak along with slightly shift in diffraction angle with respect to pure PPy. The crystalline peaks at $2\theta = 38.2^\circ$, 44.5°, 64.3° and 77.4° corresponded to Bragg's reflections from (1 1 1), (2 0 0), (2 2 0), and (3 1 1) planes of the face-centered cubic (fcc) structure of Ag. These peaks indicates crystalline nature of nanocomposite confirming inclusion of silver nanoparticles in PPy matrix. No other peaks were observed, indicating that the adopted synthesis method gives pure PPy-Ag nanocomposite [28]. The XRD data analysis using powderX [29] are given in Table 1.

The average crystalline size was calculated from the half-height width of the diffraction intense peak at 38. 2°, for PPy-Ag nanocomposite of XRD pattern using the Debye-Scherrer equation:

$$D = \frac{K\lambda}{\beta \cos\theta} \tag{2}$$

where D is the average size of the crystallite, K is the shape factor (equals 0.89 for unknown shape), λ is the wavelength of the X-ray radiation, β is the peak full line width at half of maximum (FWHM) in radian and θ is the diffraction peak position [16]. The average crystallite size of the silver is found to be about 39.67 nm, which is consistent with the result of the TEM results.

$2\theta^0$ (Intense peak)	d (A^0)	Height (Intense peak)	Area (Intense peak)	FWHM (rad)	h k l
38.2	2.3405	570.0	6840.0	0.003658	1 1 1
44.5	2.0287	196.9	3136.0	0.003903	2 0 0
64.3	1.4393	196.9	2975.0	0.004095	2 2 0
77.4	1.2286	203.0	2639.0	0.004585	3 1 1

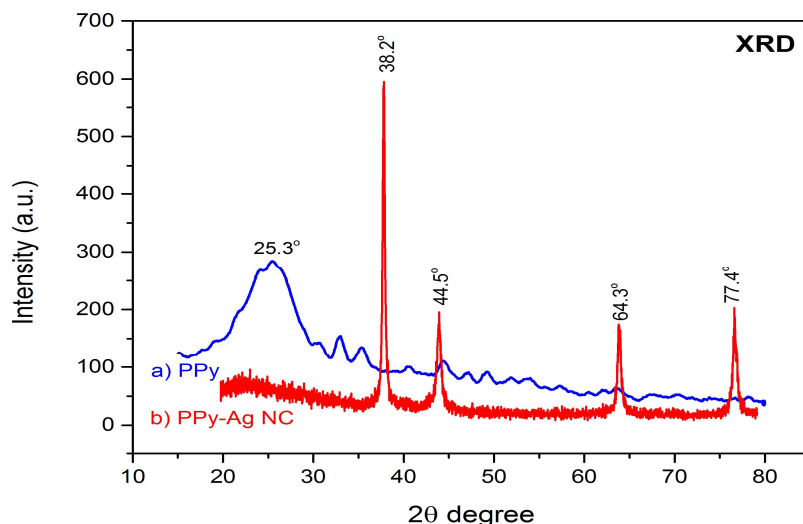Table 1: XRD data of silver nanoparticles

Fig. 6: XRD pattern of PPy and PPy-Ag nanocomposite.

E. Gas Sensing Performance

1) Selectivity of PPy-Ag nanocomposite sensor: An important parameter of gas sensors is selectivity. It can be defined as the ability of a sensor to respond to a certain gas in the presence of different gases [30]. Theoretically, the sensor should have a high response to some gases and little or no response to other gases in the same experimental conditions. Therefore, in order to study the selective behaviour of the PPy-Ag nanocomposite sensor, gas sensing measurements were carried out for various gases (NO_2, H_2S, NH_3, LPG and CO_2), each with a fixed concentration of 100 ppm and same experimental conditions. All the gas sensing measurements were carried out at room temperature and the corresponding results are shown in Fig. 7.
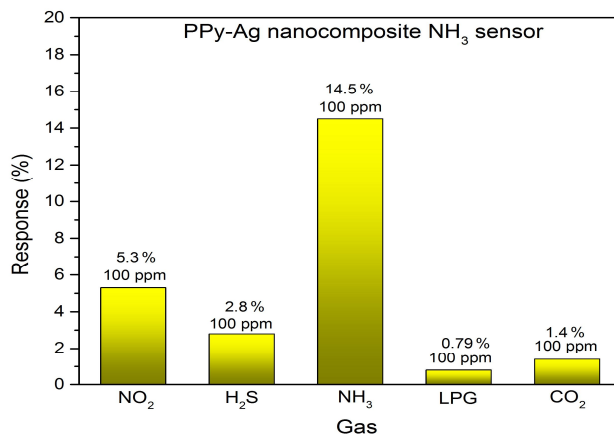
Fig. 7: Selectivity of PPy-Ag nanocomposite sensor.

In order to quantify the selectivity of NH_3, the selectivity was calculated according to definition [31]:

$$K = \frac{S_A}{S_B} \tag{3}$$

where S_A is the response of the sensor to the target gas 'A' and S_B is the response of the sensor to the other gas B.

The histogram shows that the PPy-Ag nanocomposite sensor exhibit higher response to NH_3 (14.5%), whereas it shows a considerably lower response towards NO_2, H_2S, LPG, and CO_2. It was observed that the sensor showed more selectivity for NH_3 compared to NO_2, H_2S, LPG, and CO_2. ($S_{NH3}/S_{NO2} = 2.73$, $S_{NH3}/S_{H2S} = 5.17$, $S_{NH3}/S_{LPG} = 18.35$, and $S_{NH3}/ S_{CO2} = 10.35$). Commonly the selectivity coefficient (K) of sensors should be more than five [32].

The larger value of 'K' for ammonia denotes the sensor has a better ability to differentiate the ammonia amongst mixture of gases. Therefore, we could find that the sensor has a good sensing performance when exposed to NH_3 gas. The higher response towards NH_3 than NO_2, H_2S, LPG and CO_2 can be explained on the basis of: a) Different interactions between the sensor and adsorbed gas. b) Different gases have different energies for reaction to occur on the surface of the sensor film. From the observed results, it can be concluded that the fabricated sensor is selective for NH_3 gas.

2) Sensitivity of PPy-Ag nanocomposite sensor to NH_3 gas: To test the NH_3 gas concentration characteristics, the sensor was exposed to NH_3 gas of six different concentrations at room temperature. In concentration range of 50 -500 ppm, the response of NH_3 is shown in Fig. 8. The sensitivity of the PPy-Ag nanocomposite to the concentration of the NH_3 gas at 50 ppm, 100 ppm, 200 ppm, 300 ppm, 400 ppm and 500 ppm was found to be 4.88 %, 14.57 %, 29.66 %, 38 %, 47.89 % and 53.79 % respectively. This behaviour was related to the adsorption of the NH_3 gas molecules on the surface of the PPy-Ag nanocomposite. As the concentration of NH_3 gas increased, the number of active sites for adsorption increased, leading to an increase in the sensor's response. The improved gas sensing performance of the PPy-Ag nanocomposite was due to the granular microstructure of the sensing material which offers more chemical reactions to occur at the interface [33]. PPy-Ag nanocomposite sensor gives a good response from 50 ppm concentration of NH_3 gas (4.88 %). Also, the linearity of response in the range from 50 to 500 ppm of NH_3 gas concentration suggests that the PPy sensor can be reliably used to monitor the concentration of NH_3 gas over this range.
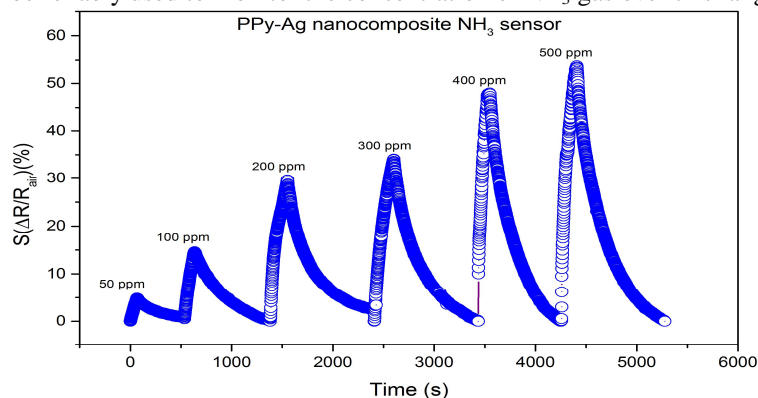

Fig. 8: Response of PPy-Ag nanocomposite sensor for various concentrations (ppm) of NH_3 gas.

Fig. 9 presents the sensitivity of PPy-Ag nanocomposite as a function of various concentrations (50-500 ppm) of NH$_3$ gas. Fig. 8 reveals that the response of PPy-Ag nanocomposite increases from 4.26 % to 20.42 % with an increase in the concentration of NH$_3$ from 50 to 500 ppm. It indicates that the sensor has a good response to NH$_3$ at room temperature. The gas response values were observed to increase continuously with increasing the gas concentration up to 500 ppm. The rate of increase of gas response is relatively higher up to 300 ppm but response reduces between 400–500 ppm leading to saturation. Thus the active region of the sensor can be considered in the range of 50–500 ppm. The linear response at lower gas concentration can be explained in terms of formation of mono-layer of gas molecules on the surface which would be expected to interact with the surface more actively giving higher response. However, at the higher gas concentration saturation in response occurs due to the formation of multi-layers of gas molecules on the sensor surface.
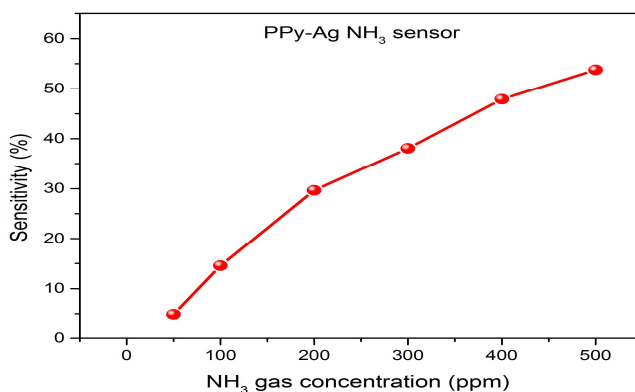

Fig. 9: Sensor response as a function of concentration (ppm) of NH$_3$ gas.

3) Sensing mechanism of PPy-Ag nanocomposite sensor: The change in the resistance of the PPy-Ag nanocomposite film as a function of time was recorded at room temperature as shown in Fig.10. Polypyrrole is a 'p' type semiconductor i.e. the predominant current carriers are holes (positive charges). In ammonia molecule, the nitrogen atom has an unshared pair of electrons. Therefore on adsorption of this gas, the holes i.e. the positive charge on the polypyrrole gets partially neutralized causing a decrease in carrier density of polypyrrole and in turn decreasing the conductance.
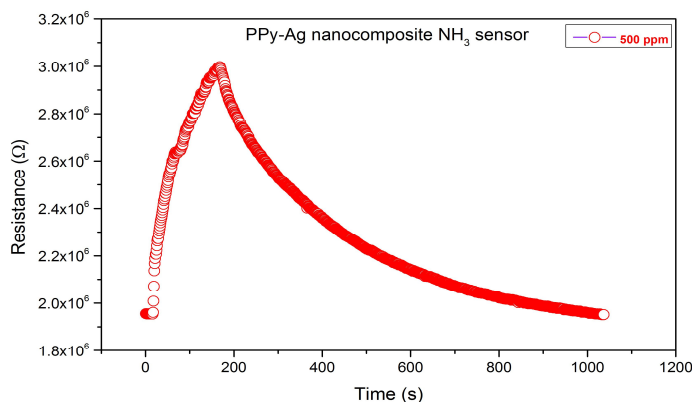

Fig.10: Change in resistance of PPy-Ag nanocomposite with respect to time on the exposure of NH$_3$ gas.

4) Reproducibility of PPy-Ag nanocomposite film sensor: Another important property of a sensor is its reversibility and reproducibility at room temperature. Fig. 11 clearly displays the reversible and reproducible response of PPy-Ag NC nanocomposite upon periodic exposure to NH$_3$. It is observed from Fig. 11 that the resistance almost recovered to its original state, which could be ascribed to the smaller size and the uniform distribution of Ag nanoparticles in the nanocomposite. The uniformly distributed Ag nanoparticles provide more uniformly distributed electron trap sites, which may result in the uniform diffusion of ammonia molecules in and out of the PPy-Ag nanocomposite. It suggested that the sensor can be used reversibly as well as reproducibly. On the basis of the above experimental results, it is indicated that the PPy-Ag nanocomposite synthesized by this method can be effectively utilized more in detecting NH$_3$ and act as an electronic nose in chemical detection of ammonia.
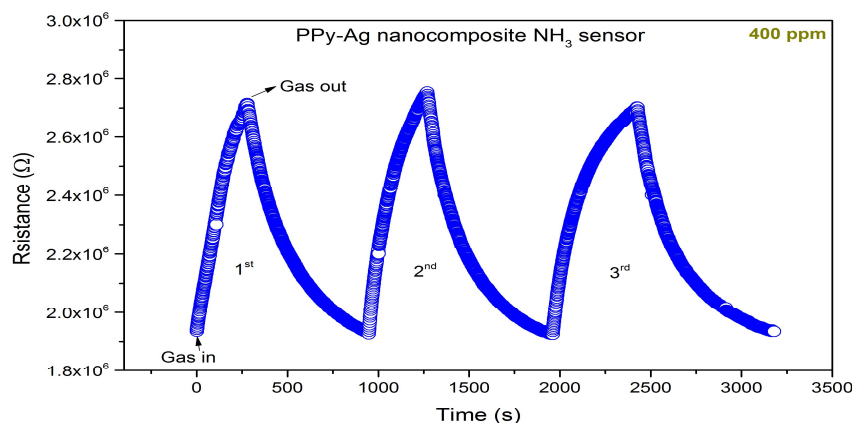
Fig.11: Repetitive response of PPy-Ag nanocomposite sensor to NH₃ gas.

5) Response and recovery times of PPy-Ag nanocomposite sensor: The response time and recovery time are crucial parameters used for characterizing a sensor.
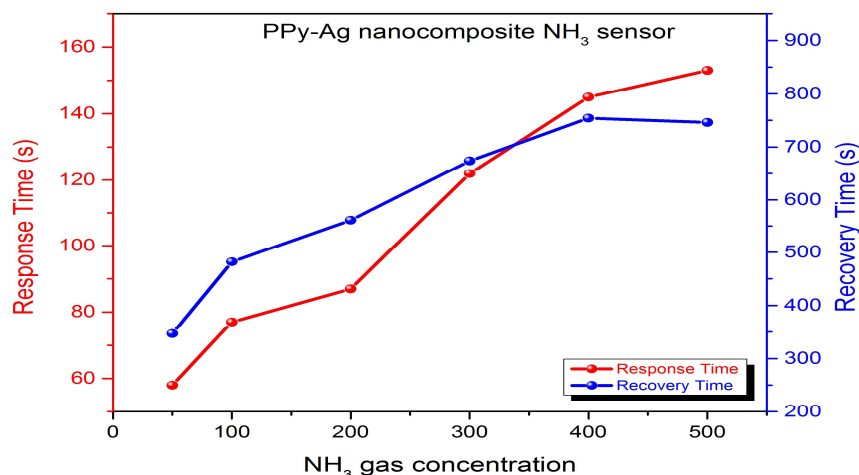

Fig.12: Response and recovery times of PPy-Ag nanocomposite film sensor for various concentrations of NH₃ gas.

Response and recovery curve of PPy-Ag nanocomposite sensor for different concentrations of NH_3 are shown in Fig. 12. From this plot, it was found that response time increased from 58 s to 153 s as the concentration of NH_3 increased from 50 ppm to 500 ppm. Such an increase in response time with increase in the concentration of NH_3 may be due to the extensive availability of vacant sites on films for gas adsorption, as evidenced by the microstructural study. The recovery time increased from 347 s to 746 s as the concentration of NH_3 increased from 50 ppm to 500 ppm which may be due to the gas reaction species that were left behind after the interaction of gas. This results in a decrease in the desorption rate and hence increases the recovery time with an increase in the concentration of NH_3.

IV. CONCLUSIONS

Polypyrrole-Silver nanocomposite has been successfully synthesized by in situ chemical oxidative polymerization based on colloidal suspension of silver nanoparticles. The presence of a series of IR characteristic bands for the PPy and PPy-Ag nanocomposite are confirmed by FTIR. TEM micrographs revealed that Spherical/semi-spherical Ag nanoparticles of about 38-60 nm were embedded in the PPy matrix. Uniform granular morphology of synthesized nanocomposite observed under SEM. XRD pattern showed broad peak at 2θ = 25.3° suggesting that PPy is amorphous, but peaks at 2θ values of 38.2°, 44.5°, 64.3° and 78.4° corresponding to cubic silver phase. The gas sensing properties of PPy-Ag nanocomposite were examined. The response of this nanocomposite, upon exposure to NH_3 gas, was observed by monitoring the change in resistance of the nanocomposite film. The sensor based on this nanocomposite, loaded with uniform and small Ag nanoparticles presents excellent reversibility and reproducibility in response. The sensor showed a quick response time of 58s and recovery time of 347s to 50 ppm of NH_3. The experimental results of NH_3 sensing studies revealed that PPy-Ag nanocomposite film acts as an practical electronic nose for NH_3 sensing at room temperature.

REFERENCES

[1] X Yang, Y Lu; Preparation of polypyrrole-coated silver nanoparticles by one-step UV-induced polymerization, Materials Letters, 2005, 59, 2484 – 2487.

[2] K F Babu, P Dhandapani, S Maruthamuthu, M A Kulandainathan; One pot synthesis of polypyrrole silver nanocomposite on cotton fabrics for multifunctional property, Carbohydrate Polymers, 2012, 90, 1557–1563.

[3] B C Sih, M O Wolf; Metal nanoparticle—conjugated polymer nanocomposites, Chem. Commun., 2005, 27, 3375–3384.

[4] Rjesha, T Ahujab, D Kumarb; Recent progress in the development of nanostructured conducting polymers/nanocomposites for sensor applications, Sensors and Actuators B, 2009, 136, 275–286.

[5] X Yanga, L Li, F Yana; Polypyrrole/silver composite nanotubes for gas sensors, Sensors and Actuators B, 2010, 145, 495–500.

[6] K H Kate, S R Damkale, P K Khanna, G H Jain; Nano-Silver Mediated Polymerization of Pyrrole: Synthesis and Gas Sensing Properties of Polypyrrole (PPy)/Ag Nano-Composite, Journal of Nanoscience and Nanotechnology, 2011, 11, 7863–7869.

[7] B Timmer, W Olthuis; A Berg, Ammonia sensors and their applications—a review, Sensors and Actuators B, 2005, 107, 666–677.

[8] A Joshi, S A Gangal, S K Gupta; Ammonia sensing properties of polypyrrole thin films at room temp, Sensors and Actuators B, 2011,156, 938– 942.

[9] D M Nerkar, S V Panse, S P Patil, S E Jaware; Development of Room Temperature Operating NH_3 Gas Sensor Based on Free Standing PPy-PVA Composite Films, International Journal of Science and Research, 2016, 5(6), 2582-2588.

[10] S T Navale, A T Mane, M A Chougule, R D Sakhare, S R Nalage, V B Patil; Highly selective and sensitive room temperature NO_2 gas sensor based on polypyrrole thin films, Synthetic Metals, 2014, 189, 94–99

[11] D M Nerkar, S E Jaware, G G Padhye; Fabrication of a Novel Flexible Room Temperature Hydrogen Sulfide (H_2S) Gas Sensor based on Polypyrrole Films, International Journal of Science and Research, 2016, 5(3), 106-111.

[12] D M Nerkar, S V Panse, S P Patil, S E Jaware, G G Padhye; Polypyrrole-silver Nanocomposite: Synthesis and Characterization, Sensors & Transducers, 2016, 202 (7), 76-82.

[13] S K Kulkarni, Nanotechnology: Principles and Practices, Springer, Third Edition, 2015, 355-358.

[14] S Jing, S Xing , L Yu , C Zhao; Synthesis and characterization of Ag/polypyrrole nanocomposites based on silver nanoparticles colloid, Materials Letters, 2007, 61, 4528-4530.

[15] S Sakthivel, A Boopathi; Synthesis and Characterization of Polypyrrole (PPy) Thin Film by Spin Coating Technique, Journal of Chemistry and Chemical Sciences, 2014, 4, 150–155.

[16] S Thakur, P P Patil; Rapid synthesis of cerium oxide nanoparticles with superior humidity-sensing performance, Sensors and Actuators B, 2014, 194, 260–268.

[17] W K Jang, J Yun, H Kim, Y S Lee; Preparation and characteristics of conducting polymer-coated multiwalled carbon nanotubes for a gas sensor, Carbon Letters, 2011,12, 162-166.

[18] S G Bachhav, D R Patil; Study of Polypyrrole-Coated MWCNT Nanocomposites for Ammonia Sensing at Room Temperature, Journal of Materials Science and Chemical Engineering, 2015, 3, 30-44

[19] M T Ramesan; Synthesis, Characterization, and Conductivity Studies of Polypyrrole/Copper Sulfide Nanocomposites, J. Appl. Polym. Sci. 2012, 128(3), 1540–1546.

[20] H K Chitte, N V Bhat, V E Walunj, G N Shinde; Synthesis of Polypyrrole Using Ferric Chloride ($FeCl_3$) as Oxidant Together with Some Dopants for Use in Gas Sensors, Journal of Sensor Technology, 2011, 1, 47–56.

[21] E Pretsch, P Buhlmann, M Badertscher; Structure determination of organic compounds tables of spectral data, Springer, 2009, Fourth Edition, pp 283.

[22] Y Wei, L Li, X Yang, G Pan, G Yan, X Yu; One-Step UV-Induced Synthesis of Polypyrrole/Ag Nanocomposites at the Water/Ionic Liquid Interface, Nanoscale Res Lett, 2010, 5, 433–437

[23] H K Chitte, N V Bhat, N S Karmakar, D C Kothari, G N Shinde; Synthesis and Characterization of Polymeric Composites Embeded with Silver Nanoparticles, World J. of Nano Science and Engineering, 2012, 2, 19–24.

[24] M A Chougule, S G Pawar, S L Patil, B T Raut, P R Godse, S Sen, V B Patil; Polypyrrole Thin Film: Room Temperature Ammonia Gas Sensor, IEEE Sensors Journal, 2011, 11, 2137–2141.

[25] H J Kharat, K P Kakde, P A Savale, K Datta, P Ghosh, M D Shirsat; Synthesis of polypyrrole films for the development of ammonia sensor, Polymers for Advanced Technologies, 2007, 18, 397–402.

[26] S Ye, Y Lu; Optical Properties of Ag@Polypyrrole Nanoparticles Calculated by Mie Theory, J. Phys. Chem. C, 2008, 112, 8767–8772.

[27] B D Cullity; Elements of X-Ray Diffraction, Addison-Wesley Publishing Company Inc., 1956, First Edition.

[28] B Li, Y Xu, J Chen, G Chen, C Zhao, X Qian, M Wang, Synthesis and characterization of Ag/PPy composite films via enhanced redox reaction of metal ions, Applied Surface Science, 2009, 256, 235–238.

[29] C Dong; PowderX: Windows-95-based program for powder X-ray diffraction data processing, J. Appl. Cryst., 1999, 32, 838.

[30] P Wadkar, D Bauskar, P Patil; High performance H2 sensor based on $ZnSnO_3$ cubic crystallites synthesized by a hydrothermal method, Talanta, 2013, 105, 327-332.

[31] M Siemons, U Simon; Gas sensing properties of volume-doped $CoTiO_3$ synthesized via polyol method, Sen. and Actuators B, 2007, 126 (2), 595–603.

[32] X Lou, S Liu, D Shi, W Chu; Ethanol-sensing characteristics of CdFe2O4 sensor prepared by sol–gel method, Materials Chemistry and Physics, 2007, 105(1), 67–70.

[33] H Tai, Y Jiang, G Xie, J Yu, , X Chen; Fabrication and gas sensitivity of polyaniline–titanium dioxide nanocomposite thin film, Sensors and Actuators B, 2007,125(2), 644–650.

INTERNATIONAL JOURNAL FOR RESEARCH

IN APPLIED SCIENCE & ENGINEERING TECHNOLOGY

Call : 08813907089 � (24*7 Support on Whatsapp)